

Deep level analysis of radiation-induced defects in Si crystals and solar cells

Masafumi Yamaguchi,^{a)} Aurangzeb Khan,^{b)} and Stephen J. Taylor
Toyota Technological Institute, 2-12-1 Hisakata, Tempaku, Nagoya 468-8611, Japan

Koshi Ando and Tsutomu Yamaguchi
Tottori University, Koyama, Tottori 680, Japan

Sumio Matsuda and Takashi Aburaya
National Space Development Agency of Japan (NASDA), 2-1-1 Sengen, Tsukuba, Ibaraki 305-8505, Japan

(Received 16 November 1998; accepted for publication 25 March 1999)

Deep level transient spectroscopy (DLTS) analysis of radiation-induced defects in p -type Si crystals and solar cells has been carried out to clarify the mechanism of the anomalous degradation of Si n^+-p-p^+ structure space cells induced by high-energy, high-fluence electron/proton irradiations. A large concentration of a minority-carrier trap with an activation energy of about 0.18 eV has been observed in irradiated p -Si using DLTS measurements, as well as the majority-carrier traps at around $E_v+0.18$ eV and $E_v+0.36$ eV. Correlations between DLTS data and solar-cell properties for irradiated and annealed Si diodes and solar cells have shown that type conversion of p -Si base layer from p -type to n -type is found to be mainly caused by introduction of the 0.18 eV minority-carrier trap center, that is, this center acts as a deep-donor center. The $E_v+0.36$ eV majority-carrier trap center is thought to also act as a recombination center that decreases minority-carrier lifetime (diffusion length). Moreover, origins of radiation-induced defects in heavily irradiated p -Si and generation of deep-donor defect has also been discussed. © 1999 American Institute of Physics. [S0021-8979(99)04813-6]

I. INTRODUCTION

Silicon was the first material used for solar cells in space and it has remained the most popular choice ever since due to its history of reliable performance. However, Si space solar cells for use in the Engineering Test Satellite-VI (ETS-VI) conducted by NASDA and launched in August 1994, have been heavily damaged by staying in the Van Allen belts.¹ Radiation testing in Si space cells has been carried out in order to clarify the mechanism on such severe radiation degradation in space. Si solar cells have shown anomalous behavior such as an increase in short-circuit current I_{sc} and decrease in open-circuit voltage V_{oc} , followed by an abrupt decrease of I_{sc} and cell failure, under high fluence irradiation with high-energy electrons or protons. We have proposed a model² to explain these phenomena by expressing the change in carrier concentration of the base region, in addition to the well-known model,³ where short-circuit current is decreased by minority-carrier lifetime (diffusion length) reduction with irradiation. However, the origins of radiation-induced defects responsible for carrier removal and reduction in minority-carrier lifetime (diffusion length) in Si are not yet clearly understood.

In this paper, properties of radiation-induced defects and generation of deep-donor defects in heavily irradiated p -type Si have been studied using deep level transient spectroscopy (DLTS), capacitance–voltage ($C-V$), and Hall measurements. Correlations between DLTS data and solar-cell prop-

erties for irradiated and annealed Si diodes and solar cells have shown that type conversion of the p -Si base layer is found to be mainly caused by introduction of the 0.18 eV minority-carrier trap center. The $E_v+0.36$ eV majority-carrier trap center is found to also act as a recombination center. Moreover, origins of radiation-induced defects in irradiated p -Si have also been discussed.

II. EXPERIMENTAL PROCEDURE

The samples used in this study were backsurface field and reflector (BSFR) structure n^+-p-p^+ Si space solar cells and diodes with p -base layer resistivity of around $10\ \Omega\text{ cm}$ (base doping concentration of $(1-2)\times 10^{15}\text{ cm}^{-3}$) and junction depth of $0.15\ \mu\text{m}$ as shown in Fig. 1. In the cell and diode fabrication, B-doped Si single crystals grown by the Czochralski (CZ) method were used and n^+-p-p^+ back-surface field (BSF) layers were made by thermal diffusion of P and B. Cell and diode thickness was $50\ \mu\text{m}$. Typical initial values of short-circuit current (I_{sc}), open-circuit voltage (V_{oc}), and conversion efficiency of the $2\times 2\text{ cm}^2$ solar cell under air mass 0 (AM0) condition were 160 mA, 605 mV, and 14%, respectively.

The samples were irradiated in the open-circuit condition with 1 MeV electrons using a Cockroft–Walton accelerator, taking care to avoid sample heating by appropriate control of the beam current and water cooling of the sample mount. Fluences of 1 MeV electrons ranged from 1×10^{14} to $2\times 10^{17}\text{ cm}^{-2}$. Solar-cell properties were measured under the AM0 spectrum using a solar simulator. DLTS, $C-V$ and Hall measurements were also carried out to clarify the ori-

^{a)}Electronic mail: masafumi@toyota-ti.ac.jp

^{b)}Electronic mail: a.khan@toyota-ti.ac.jp

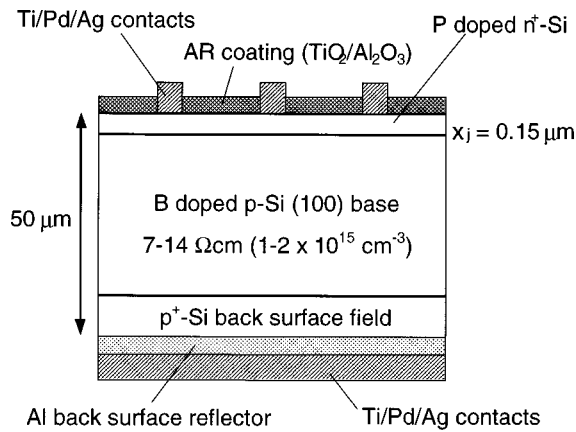


FIG. 1. A schematic diagram of a Si space solar cell or diode used in this study.

gins of radiation-induced defects and the mechanism on severe radiation degradation of Si cells. A mesa area of $2.56 \times 10^{-6} \text{ m}^2$ was defined in order to keep the capacitance of the device within the range of the capacitance meter used for $C-V$ and DLTS measurements (Sanwa MI416B operating at a measurement frequency of 1 MHz). DLTS measurements were performed at temperatures from 140 to 190 °C, which represents the full range of our instrument in its present configuration, with samples mounted on indium foil to ensure good thermal contact with the cryostat. The temperature measured by the system thermocouple during the DLTS experiments was checked by comparison with an additional thermocouple attached with silver paste to a piece of silicon in place of the sample. This temperature difference was less than 2 °C at all the scan speeds employed in these measurements. The diode bias was switched between a quiescent level of $-2-0 \text{ V}$ during the fill pulse of 1 ms duration, which was checked to be long enough to saturate the traps.

Annealing was either performed under primary vacuum in the sample cryostat (for temperatures up to 200 °C) or in an electric furnace (for temperatures $>200 \text{ °C}$) under nitrogen gas flow.

III. BRIEF EXPLANATION OF THE MODEL PROPOSED FOR THE ANOMALOUS RADIATION DEGRADATION OF SI CELLS

Figure 2 shows comparison of experimental results for short-circuit current degradation of Si space cells with 1 MeV electron irradiation and analytical results calculated by the model proposed. A gradual degradation of Si cell properties with fluence has been observed under lower fluence irradiation below 10^{16} cm^{-2} . An anomalous increase of short-circuit current I_{sc} has been observed under intermediate fluence region from $2 \times 10^{16} \text{ cm}^{-2}$ to about $5 \times 10^{16} \text{ cm}^{-2}$, and an abrupt decrease in I_{sc} and failure of Si cells have been observed under higher fluence irradiation above $5 \times 10^{16} \text{ cm}^{-2}$.

A mechanism on anomalous radiation degradation of Si space solar cells induced with wide ranges of fluence electron or proton irradiations has been proposed.² As it is well known, a gradual degradation of Si cell properties with flu-

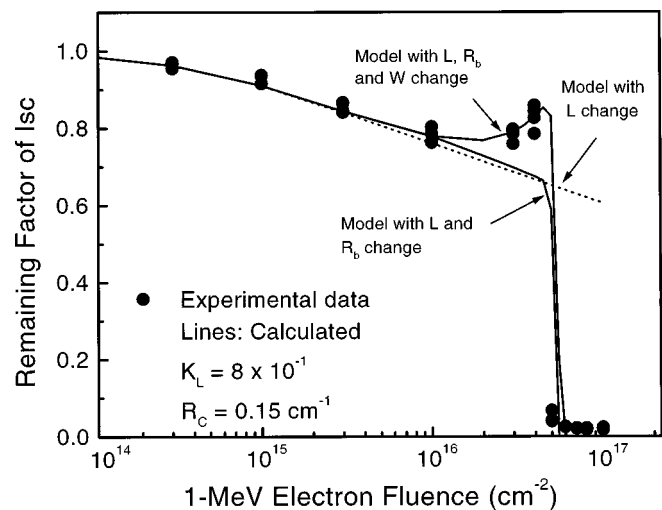


FIG. 2. Comparison of experimental results for short-circuit current degradation of Si cells with 1 MeV electron irradiation and analytical results calculated by considering mechanisms: (1) minority-carrier diffusion length decrease, (2) depletion layer broadening, and (3) carrier concentration decrease with irradiation.

ence below 10^{16} cm^{-2} is understood by minority-carrier diffusion length (lifetime) degradation³ with high-energy electron or proton irradiation. Recombination centers tend to affect the solar-cell performance by reducing the minority-carrier diffusion length of electrons in the p -type base, L , (or equivalently lifetime, τ , using $L = (D\tau)^{1/2}$) from the pre-irradiation value L_0 to a post-irradiation value L_ϕ through

$$\Delta(1/L^2) = 1/L_\phi^2 - 1/L_0^2 = \sum I_{ri} \sigma_i v \phi / D = K_L \phi, \quad (1)$$

where, I_{ri} is the introduction rate of i th recombination center by irradiation, σ_i is the capture cross section of minority-carrier by i th recombination center, v is the thermal velocity of minority-carrier, D is the minority-carrier diffusion coefficient, K_L is the damage coefficient for minority-carrier diffusion length, and ϕ is the fluence.

Figure 3 shows the comparison of experimental results for short-circuit current degradation of Si space cells under low fluence of 1 MeV electron irradiation and analytical re-

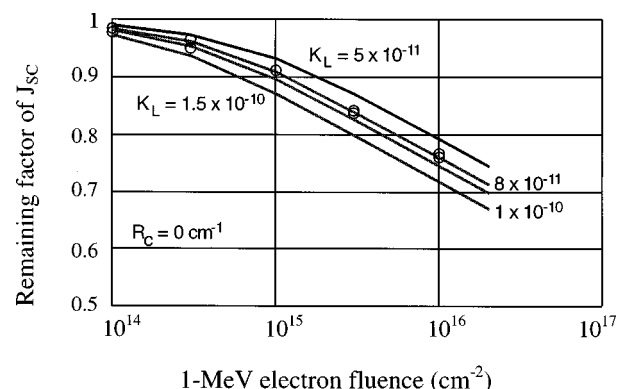


FIG. 3. Comparison of experimental results for short-circuit current degradation of Si space cells under low fluence of 1 MeV electron irradiation and analytical results calculated results by changing values of the damage coefficient for minority-carrier diffusion length K_L .

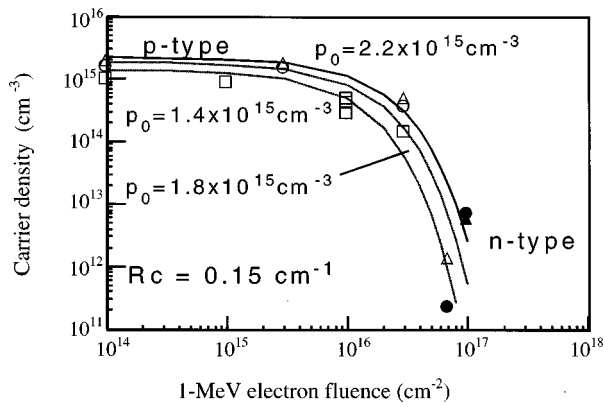


FIG. 4. Calculated and experimental changes in carrier concentration of p -Si crystals with carrier concentrations of 1.4×10^{15} , 1.8×10^{15} , and $2.2 \times 10^{15} \text{ cm}^{-3}$, as a function of 1 MeV electron fluence.

sults calculated by changing the value of the damage coefficient for minority-carrier diffusion length, K_L . From fitting to experimental results, K_L was determined to be 8×10^{-11} for 1 MeV electron irradiation. This value is almost the same as the value⁴ reported previously for p -Si with a resistivity of about $10 \Omega \text{ cm}$.

As a mechanism for the abrupt decrease in I_{sc} of Si cells observed under higher fluence irradiation above $5 \times 10^{16} \text{ cm}^{-2}$, a decrease in carrier concentration and increase in resistivity of p -type base layer have been proposed.² Figure 4 shows calculated and experimental changes in carrier concentration of p -Si crystals with carrier concentrations of $1.4 \times 10^{15} \text{ cm}^{-3}$, $1.8 \times 10^{15} \text{ cm}^{-3}$, and $2.2 \times 10^{15} \text{ cm}^{-3}$, as a function of 1 MeV electron fluence. Carrier concentrations of p -Si before and after irradiation were measured using the C - V method and Hall effect. Majority-carrier traps induced by irradiation reduce the base-carrier concentration: the change in carrier concentration Δp in p -Si layer with radiation fluence is expressed by³

$$\Delta p = p_0 - p_\phi = \sum I_{ij} f(E_{ij}) \phi \sim R_c \phi, \quad (2)$$

where I_{ij} is introduction rate of j th majority-carrier trap center by electron irradiation, $f(E_{ij})$ the capture rate of majority-carrier by j th majority-carrier trap center, and R_c the carrier removal rate by irradiation. The carrier concentration p_ϕ in p -Si layer after irradiation is approximated from Eq. (2) as follows:

$$p_\phi = p_0 \exp(-R_c \phi / p_0). \quad (3)$$

As can be seen in Fig. 4, a remarkable decrease in carrier concentration in the p -Si base layer has been observed and the carrier removal rate R_c determined from the curve fitting for 1 MeV electron irradiated p -Si layer is about 0.15 cm^{-1} . As a result of a decrease in the carrier concentration in the p -Si layer with electron irradiation, a significant increase in series resistance of the Si solar cell is induced. Therefore, an increase in series resistance of the Si cell is thought to cause a decrease in short-circuit current and to the abrupt failure of the Si cell. Moreover, type conversion of p -type Si from p -type to n -type has been observed under the higher fluence irradiation above $5 \times 10^{16} \text{ cm}^{-2}$, as shown in Fig. 4. A change from $n^+ - p - p^+$ structure to $n^+ - n - p^+$ structure

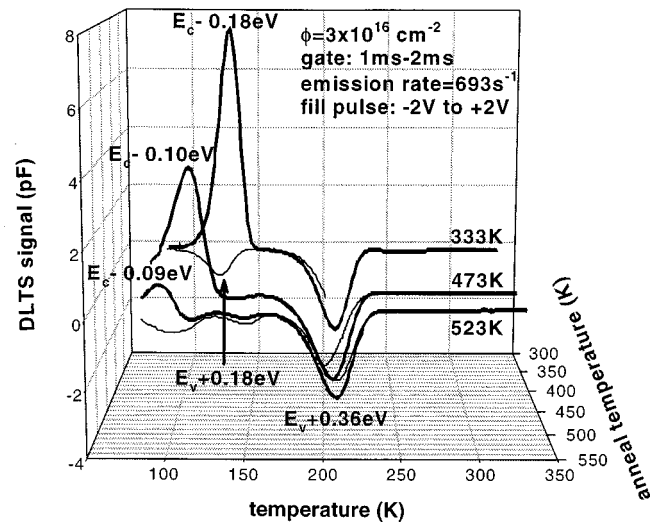


FIG. 5. DLTS spectra of a Si diode irradiated with $3 \times 10^{16} \text{ cm}^{-2}$ 1 MeV electrons as a function of annealing temperature. For clarity, spectra at only three temperatures are included.

due to type conversion of the p -Si layer in Si solar cells under high fluence irradiation has also been confirmed⁵ using the electron-beam-induced current method.

Furthermore, as a mechanism for the anomalous increase of short-circuit current observed in the intermediate fluence region from $2 \times 10^{16} \text{ cm}^{-2}$ to about $5 \times 10^{16} \text{ cm}^{-2}$, depletion layer broadening with irradiation has been proposed.² An increase in short-circuit current density J_{sc} due to depletion layer broadening is expressed by

$$J_{sc} \sim 1 - \exp(-\alpha W), \quad (4)$$

where, α is optical absorption coefficient and W the width of depletion layer.

It can be seen in Fig. 2, that good correlation between the calculated and experimental results for short-circuit current degradation of Si space cells with 1 MeV electron irradiation shows the validity of the analytical model.

IV. DLTS ANALYSIS OF RADIATION-INDUCED DEFECTS IN Si

In order to clarify the origins of radiation-induced defects in Si and correlation between their behavior and Si solar cell properties, DLTS analysis has been carried out. Figure 5 shows both the majority- and minority-carrier DLTS spectra of a Si diode irradiated with $3 \times 10^{16} \text{ cm}^{-2}$ 1 MeV electrons as a function of annealing temperature. A large concentration of a minority-carrier trap with an activation energy of about 0.18 eV has been observed, as well as the majority-carrier traps at around $E_v + 0.18$ and $E_v + 0.36$ eV. The defect at $E_v + 0.18$ eV has previously been identified^{6,7} as the di-vacancy,⁸ $V-V^+(E_v + 0.18-0.23 \text{ eV}, \sigma \approx 3 \times 10^{-16} \text{ cm}^2)$.

The $E_v + 0.36$ eV defect has previously been proposed to be due to a combination of two traps⁹⁻¹¹ at around $E_v + 0.36$ eV, a fast component identified with the $V-C-O$ complex ($E_v + 0.34 \text{ eV}, \sigma \approx 1.1 \times 10^{-16} \text{ cm}^2$) and a slow component identified with the C_s-C_i complex ($E_v + 0.37$

TABLE I. Trap levels E_a , introduction rates I_t , cross sections σ and possible identifications of defects induced by 1 MeV electrons.

E_a (eV)	I_t (cm ⁻¹)	σ (cm ²)	Possible identification
$E_v + 0.18$	0.003	8.9×10^{-17}	V-V ⁺
$E_v + 0.30$ (after annealing at 200 °C)	0.0008	7.3×10^{-15}	V-C-O/V-O-B/ C _s -Ci/C-Si _i
$E_v + 0.36$	0.007	7.2×10^{-16}	C _i -O _i /B _i -O _i
$E_c - 0.18$	0.013	1.8×10^{-16}	V-V(---)/O _i -B _i

eV, $\sigma \approx 8 \times 10^{-18}$ cm²). The identification of this level with C-O-V¹⁶ complex is ruled out by electron paramagnetic resonance (EPR) measurements which suggested it to be the interstitial-carbon-interstitial-oxygen complex (C_i-O_i).¹² Moreover, a detailed study,¹³ based on EPR investigation combined with DLTS on electron-irradiated Si has strongly negated the association of this level with the C_i-C_s center in favor of the C_i-O_i defect. Thus, this level is generally identified with the C_i-O_i complex. We concluded that at least one of component of this level is associated with the C_i-O_i complex, as previously discussed, and another component may be a boron-related defect such as B_i-O_i.

The activation energy and emission rates of electron trap at $E_c - 0.18$ eV are almost identical to the E1 trap reported by Kimerling⁶ and Mooney *et al.*¹¹ Watkins and Corbett¹⁴ had observed a same kind of level known as A-center (vacancy-oxygen complex) in *n*-type Si. Following Mooney *et al.*,¹¹ one possible candidate of this level is interstitial-boron-interstitial-oxygen (B_i-O_i) complex which transforms to a vacancy oxygen boron (V-O-B) complex upon annealing to the result of $H(0.30$ eV) level in our study. The other possible candidate for this level is the V-V(---) state of the di-vacancy defect.⁶ Table I shows trap levels E_a , introduction rates I_t , cross sections σ , and possible identifications of defect centers, measured by DLTS, in CZ-grown *p*-Si induced with 1 MeV electrons. However, their microscopic origins are still unclear at present.

The concentrations of the different traps measured by DLTS are compared to the change in carrier concentration in Fig. 6. Although the introduction rates of the individual majority-carrier traps are different for electron and proton irradiated samples, the total majority-carrier trap introduction rate expressed as a function of effective 1 MeV electron dose¹⁵ is the same. The total concentrations of these majority-carrier traps and the minority-carrier trap at around $E_c - 0.18$ eV have been found to be nearly equal to the change in carrier concentrations. The $E_v + 0.18$ eV defect was coherent with the properties expected of the dominant compensating center, but the observed concentration of this trap was too low to account for the estimated reduction in carrier concentration. In contrast, the concentration of the minority-carrier trap at around $E_c - 0.18$ eV, which also decreased as the carrier concentration of the diodes increased, was high enough to be responsible for most of the observed compensation and subsequently type conversion of the base layer from *p*- to *n*-type. The $E_v + 0.36$ eV defect is thought to be responsible for minority-carrier lifetime (diffusion length)

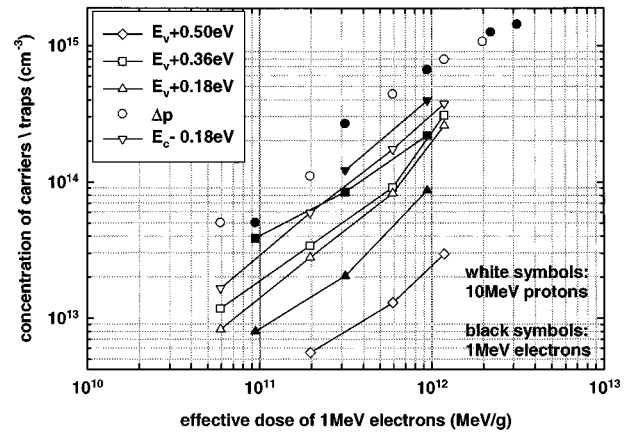


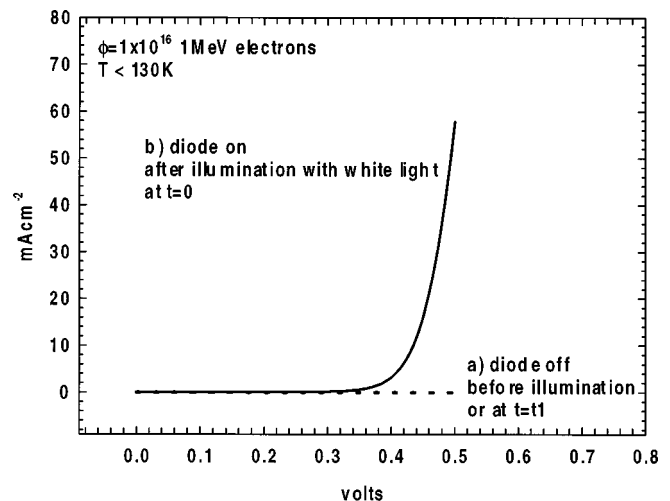
FIG. 6. Comparison of the introduction rates of the defects illustrated in Fig. 5 together with the change in the base carrier concentration of the same samples measured by C-V profile at 300 K.

degradation according to the annealing experiments in the higher temperature range as will be described. This means that the $E_v + 0.36$ eV is thought to act as a recombination center, in addition to a role as a majority-carrier trap center.

V. GENERATION OF DEEP-DONOR STATE DEFECT RESPONSIBLE FOR TYPE CONVERSION

The $E_c - 0.18$ eV defect center has been shown¹⁶ to be responsible for type conversion by observing the I - V characteristics of the Si diodes as a function of measurement temperature.

As the diodes were maintained at forward bias and cooled, a normal rectifying characteristic was observed until a critical temperature at which oscillation between on and off states was observed and below which there was no conduction, as illustrated in Fig. 7. The critical temperature, typically 130 K for a diode irradiated with 1×10^{16} cm⁻² 1 MeV electrons, varied from sample to sample due to variations in

FIG. 7. I - V characteristic of a diode irradiated with a fluence of 1×10^{16} 1 MeV electrons cm⁻² (a) in the off state below 130 K before illumination with white light and subsequently a time $t = t_1$ after illumination and (b) at time $t = 0$ immediately after illumination.

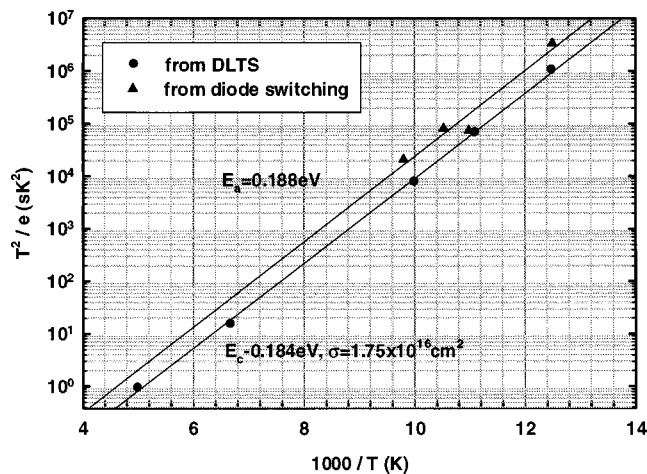


FIG. 8. Arrhenius plot showing data from both the DLTS spectrum and as deduced from the switching properties of the diode as a function of temperature.

the trap concentration. If the sample was cooled further and then briefly illuminated with which light, conduction was restored for a time interval, which was temperature dependent.

The compensation of the p -type base layer is likely to be caused by the introduction of deep-donor defect D^+ , which is positively charged before electron capture. If the compensation of the p -type layer is assumed to be caused by a concentration N_T of a unique donor level D , then under white light bias in the steady state, conduction must be facilitated by electron capture on this trap as described by



which turns the diode on.

Subsequently, when the light bias is removed at time $t = 0$, the capture rate falls to zero and captured electrons are reemitted to the conduction band at a rate, e , as the system returns to equilibrium. The traps, which are now positively charged, compensate the base layer and turn the diode off. That is, the diode switching from on to off states is thought to be related to electron emission from a neutral state of the deep-donor defect and changes in concentration of neutral defects, N_T^0 , is expressed by

$$N_T^0 = N_T \exp(-et). \quad (6)$$

Therefore, in the same way as we use the DLTS data to plot emission rate e as a function of absolute temperature T for different traps, we can construct an Arrhenius plot by measuring at different temperatures the time interval, t_1 , taken for the neutral defect N_T^0 to fall to the critical value at which diode switching occurs. This allows us to obtain the value of E_a for the dominant trap. Figure 8 compares data from both the DLTS measurement for the minority-carrier trap and the diode switching experiments. The two activation energies are the same, within experimental error. This result indicates that the minority-carrier trap at $E_c - 0.18$ eV acts as a deep-donor center, which compensates the diodes.

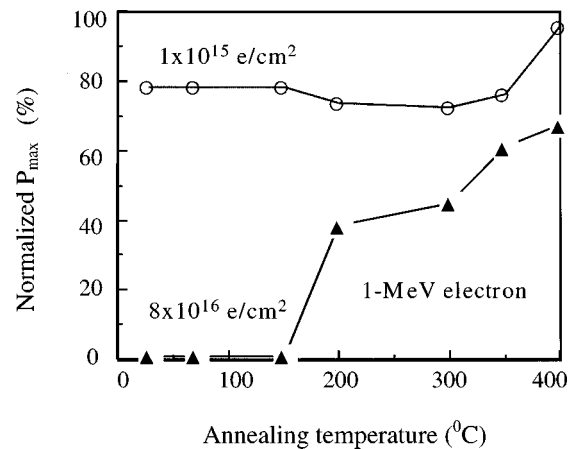


FIG. 9. Isochronal (10 min) annealing recovery of maximum output power of Si solar cells irradiated with 1 MeV 1×10^{15} and 8×10^{16} cm^{-2} electrons.

VI. ANNEALING BEHAVIORS OF RADIATION-INDUCED DEFECTS IN Si CRYSTALS AND SOLAR CELLS

Figure 9 shows isochronal (10 min) annealing recovery of maximum output power of Si solar cells irradiated with 1 MeV electrons. The lower fluence ($1 \times 10^{15} \text{ cm}^{-2}$) irradiated Si cell whose degradation is mainly caused by a decrease in minority-carrier diffusion length has a reverse annealing stage at 200–300 °C and a recovery stage at around 350 °C. Annealing behavior of solar cell properties observed in the lower fluence irradiated Si cell is quite similar with that observed by Weinberg and Swartz.¹⁷ On the other hand, the higher fluence ($8 \times 10^{16} \text{ cm}^{-2}$) irradiated sample whose degradation is mainly caused by a decrease in carrier concentration of base layer, has two recovery stages at around 200 and 350 °C.

Figure 10 also shows isochronal (10 min) annealing recovery of the minority-carrier trap center at around $E_c - 0.18$ eV and majority-carrier trap centers at around $E_v + 0.18$ eV and $E_v + 0.36$ eV, measured by DLTS, in p -type Si irradiated

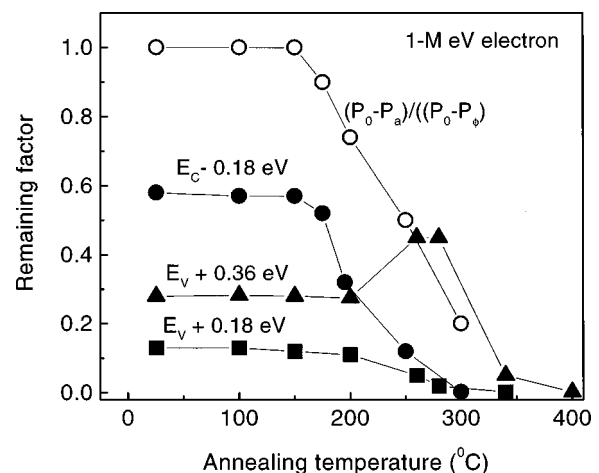


FIG. 10. Comparison of isochronal (10 min) annealing of densities of $E_c - 0.18$ eV, $E_v + 0.18$ eV and $E_v + 0.36$ eV defect centers measured by DLTS with that of carrier concentration of p -type Si irradiated with 1 MeV electrons.

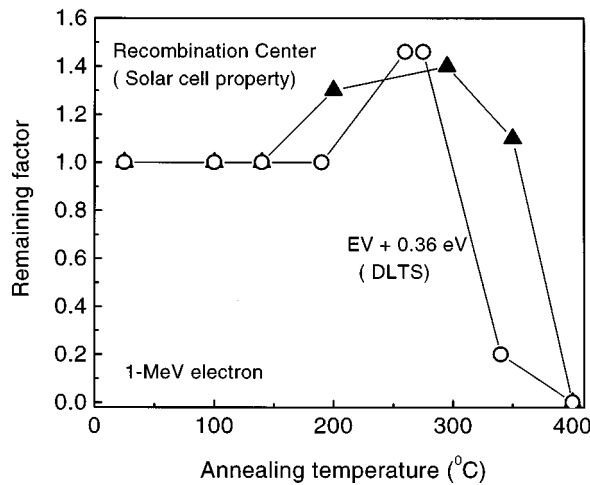


FIG. 11. Comparison of isochronal (10 min) annealing of the majority-carrier trap at $E_v + 0.36$ eV measured by DLTS with that of the dominant recombination center determined by solar-cell properties in p -type Si irradiated with 1 MeV electrons.

with 1 MeV electrons. The minority-carrier trap at $E_c - 0.18$ eV and the majority-carrier trap at $E_v + 0.18$ eV are found to have an annealing stage at around 200 and 250 °C, respectively. On the other hand, the majority-carrier trap center at $E_v + 0.36$ eV has a reverse annealing stage at 200–300 °C and a recovery stage at around 350 °C. In this figure, changes in the relative majority-carrier trap density with annealing were also estimated by changes in carrier concentration according to the following equation:

$$N_{Ta}/N_{T\phi} = (p_0 - p_a)/(P_0 - P_\phi), \quad (7)$$

where suffix a shows after annealing. It can be seen in Fig. 10 that annihilations of the minority-carrier trap at $E_c - 0.18$ eV and the majority-carrier trap at $E_v + 0.18$ eV with an annealing stage of 200–250 °C are thought to cause a recovery of carrier concentration in p -type Si.

Figure 11 also compares isochronal (10 min) annealing of density of the majority-carrier trap at $E_v + 0.36$ eV measured by DLTS and recombination center determined by solar cell properties in p -type irradiated with 1 MeV electrons. In Fig. 11, changes in the relative recombination center density N_r with annealing were also estimated by changes in short-circuit current density J_{sc} of the solar cell according to the following:

$$N_{ra}/N_{r\phi} \sim L_\phi^2(L_0^2 - L_a^2)/[L_a^2(L_0^2 - L_\phi^2)] \\ \sim J_{sc\phi}^2(J_{sc0}^2 - J_{sca}^2)/[J_{sca}^2(J_{sc0}^2 - J_{sc\phi}^2)]. \quad (8)$$

It can be seen in Fig. 11 that features of the $E_v + 0.36$ eV majority-carrier trap center with a reverse annealing stage at 200–300 °C and a recovery stage at around 350 °C are similar to the changes in minority-carrier diffusion length L determined by solar cell properties. That implies that the $E_v + 0.36$ eV majority-carrier trap center may also act as a recombination center. However, the possibility that other mid-gap levels may dominate the minority-carrier lifetime cannot be discounted, since these traps are difficult to measure at all (due to their signal typically being at the extreme limit of the

measurable DLTS spectrum) and a relatively small concentration of mid-gap level traps can have a large effect.

VII. DISCUSSION

Table I summarizes trap levels, introduction rates, cross sections, and possible identifications of defects in p -type Si induced by 1 MeV electrons.

A recovery stage for solar-cell properties at around 200 °C is found to be related to carrier concentration recovery that is attributed to annihilations of the minority-carrier trap at $E_c - 0.18$ eV and the majority-carrier trap at $E_v + 0.18$ eV.

The origin of the majority-carrier trap at around $E_v + 0.18$ eV is thought to be di-vacancy (V–V),⁸ as it is well known. Although the annealing stage for the di-vacancy determined by Watkins and Corbett⁸ is 270 °C in CZ-Si and 350 °C in floating zone-Si (FZ-Si), respectively, that for the majority-carrier trap at around $E_v + 0.18$ eV observed in this study is 200–250 °C. Furthermore, they observed the stress-induced di-vacancy axis polarization⁸ during annealing at around 150 °C. Further study is necessary to solve the disagreement for annealing behavior of the $E_v + 0.18$ eV defect center.

In this study, the $E_c - 0.18$ eV minority-carrier trap center is found to also act as deep-donor center and to be responsible for type conversion of p -Si. The activation energy and emission rates of electron trap center at $E_c - 0.18$ eV is similar to the signal to the $E1$ trap center reported by Kimerling⁶ attributed this signal to the A-center (vacancy-oxygen complex) which had previously been assigned in n -type Si by Watkins and Corbett¹⁴ as a transition from the neutral to the negative charged state of a vacancy-oxygen complex. However, their annealing behaviors are very different. While the annealing stage of the A-center determined by Corbett et al.¹⁸ is 300 °C, that of the electron trap center at $E_c - 0.18$ eV observed in our study is 200 °C. However, our explanation requires that compensation should be caused by a center which is positively charged before electron capture, whereas A-center is proposed to be neutral before electron capture.¹⁴ The di-vacancy⁸ and O_i – B_i complex defect¹¹ may also be a possible candidate for the $E_c - 0.18$ eV minority-carrier trap center.

As the $E_c - 0.18$ eV minority-carrier trap center disappear, the $E_v + 0.30$ eV majority-carrier trap center is observed to be appeared. The possible identifications for the $E_v + 0.30$ eV trap center reported are V–O–B,¹¹ V–C–O,¹⁰ C_s–C_i¹⁰ and C–Si_i.¹⁰

On the other hand, a recovery stage at around 350 °C is found to related to minority-carrier diffusion length recovery that is due to annihilation of the majority-carrier trap center at around $E_v + 0.36$ eV that acts as a recombination center. The origin of the $E_v + 0.36$ eV majority-carrier trap is still a matter of discussion; however, this level is generally identified with the C_i–O_i complex.¹³

Figure 12 shows changes in damage coefficient K_L for minority-carrier diffusion length, measured with 1 MeV electron irradiation in CZ-grown and FZ-grown p -Si as a function of carrier concentration. It can be seen Fig. 12, that

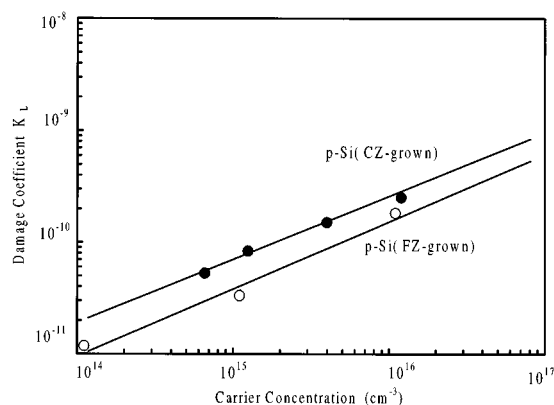


FIG. 12. Changes in damage coefficient K_L for minority-carrier diffusion length, measured with 1 MeV electron irradiation in CZ-grown and FZ-grown p -Si as a function of carrier concentration.

K_L values increase with an increase in boron concentration and oxygen concentration in p -type Si. Figure 12 suggests that the recombination center responsible for the minority-carrier diffusion length degradation must be boron- and oxygen-related defect and thus the V–O–B complex defect may be a possibility.

However, the microscopic origins of the above defects are still unclear at present. Further study is necessary.

VIII. SUMMARY

DLTS analysis of radiation-induced defects in p -type Si crystals and solar cells was carried out to clarify the mechanism on an anomalous degradation of Si $n^+ - p - p^+$ structure space cells induced by high-energy, high-fluence electron/proton irradiations. A large concentration of the $E_c - 0.18$ eV minority-carrier trap was observed in irradiated p -Si using DLTS measurements, as well as the $E_v + 0.18$ eV and $E_v + 0.36$ eV majority-carrier traps. Correlations between DLTS data and solar-cell properties for irradiated and annealed samples have shown that type conversion of p -Si base layer from p -type to n -type is found to be mainly caused by introduction of the 0.18 eV minority-carrier trap center, that

is, this center acts as a deep-donor center. The $E_v + 0.36$ eV majority-carrier trap center is thought to also act as a recombination center that decreases minority-carrier diffusion length. Moreover, the origins of radiation-induced defects in heavily irradiated p -Si were also discussed.

ACKNOWLEDGMENTS

The authors would like to thank the members of the Committee for Study of Solar Cell Radiation Damage Mechanism for their fruitful discussion. This work was partly supported by the Ministry of Education as a Private University High-Technology Research Center Program.

- ¹Y. Yamamoto, O. Kawasaki, S. Matsuda, and Y. Morita, in *Proceedings of the European Space Power Conference*, Poitiers, France, 4–8 September 1995, ESA SP-369 (1995), pp. 573–578.
- ²M. Yamaguchi, S. J. Taylor, S. Matsuda, and O. Kawasaki Appl. Phys. Lett. **68**, 3141 (1996).
- ³M. Yamaguchi and C. Amno, J. Appl. Phys. **57**, 537 (1985).
- ⁴H. Y. Tada, J. R. Carter, B. E. Anspaugh, and R. G. Downing, JPL, Publication No. 82-69, 1982.
- ⁵S. J. Taylor, M. Yamaguchi, M. J. Yang, M. Imaizumi, S. Matsuda, and O. Kawasaki, Appl. Phys. Lett. **70**, 2165 (1997).
- ⁶L. C. Kimerling, IEEE Trans. Nucl. Sci. **NS-23**, 1497 (1976).
- ⁷G. Ferenczi, C. A. Londos, T. Pavelka, M. Somogyi, and A. Mertens, J. Appl. Phys. **63**, 183 (1988).
- ⁸G. D. Watkins and J. W. Corbett, Phys. Rev. **138**, 543 (1965).
- ⁹J. Vanhellemont, E. Simoen, C. Claeys, A. Kaniava, E. Gaubas, G. Bosman, B. Johlander, L. Adams, and P. Clauws, IEEE Trans. Nucl. Sci. **NS-41**, 1924 (1994).
- ¹⁰Y. H. Lee, L. J. Cheng, J. D. Gerson, P. M. Mooney, and J. W. Corbett, Solid State Commun. **21**, 109 (1977).
- ¹¹P. M. Mooney, L. J. Cheng, N. Suli, J. D. Gerson, and J. W. Corbett, Phys. Rev. B **15**, 3836 (1977).
- ¹²J. M. Trombetta and G. D. Watkins, Appl. Phys. Lett. **51**, 1103 (1987).
- ¹³L. W. Song, X. D. Zham, B. W. Benson, and G. D. Watkins, Phys. Rev. B **42**, 5765 (1990).
- ¹⁴G. D. Watkins and J. W. Corbett, Phys. Rev. **121**, 1001 (1961).
- ¹⁵G. P. Summers, R. J. Walters, M. A. Xapsos, E. A. Burke, S. R. Messenger, P. Shapiro, and R. L. Slater, in *Proceedings of the First World Conference on Photovoltaic Energy Conversion* (IEEE, New York, 1994), p. 2068.
- ¹⁶T. Yamaguchi, S. J. Taylor, S. Watanabe, K. Ando, M. Yamaguchi, T. Hisamatsu, and S. Matsuda, Appl. Phys. Lett. **72**, 1226 (1998).
- ¹⁷I. Weinberg and C. K. Swartz, Appl. Phys. Lett. **36**, 693 (1980).
- ¹⁸J. W. Corbett, G. D. Watkins, and R. S. McDonald, Phys. Rev. A **135**, 1381 (1964).